Accepted Manuscript

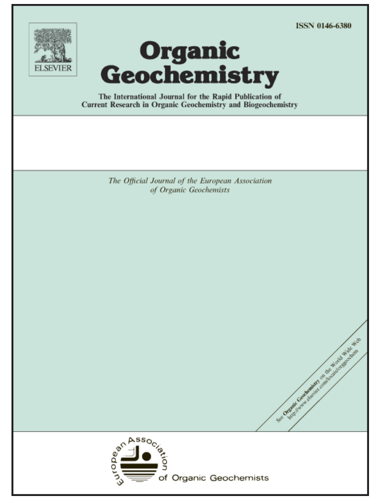

Glacial-interglacial vegetation changes in northeast China inferred from isotopic composition of pyrogenic carbon from Lake Xingkai sediments

Weiwei Sun, Enlou Zhang, Enfeng Liu, Jie Chang, Rong Chen, Ji Shen

PII: S0146-6380(18)30047-0
DOI: https://doi.org/10.1016/j.orggeochem.2018.03.004
Reference: OG 3694

To appear in: *Organic Geochemistry*

Received Date: 27 September 2017
Revised Date: 5 March 2018
Accepted Date: 6 March 2018

Please cite this article as: Sun, W., Zhang, E., Liu, E., Chang, J., Chen, R., Shen, J., Glacial-interglacial vegetation changes in northeast China inferred from isotopic composition of pyrogenic carbon from Lake Xingkai sediments, *Organic Geochemistry* (2018), doi: https://doi.org/10.1016/j.orggeochem.2018.03.004

Glacial-interglacial vegetation changes in northeast China inferred from isotopic composition of pyrogenic carbon from Lake Xingkai sediments

Weiwei Sun[a*], Enlou Zhang[a], Enfeng Liu[b], Jie Chang[a], Rong Chen[a], Ji Shen[a, c*]

[a] *State Key Laboratory of Lake Science and Environment, Nanjing Institute of Geography and Limnology, Chinese Academy of Sciences, Nanjing 210008, China*

[b] *College of Geography and Environment, Shandong Normal University, Jinan 250014, China*

[c] *College of Earth Sciences, University of Chinese Academy of Sciences, Beijing 100049, China*

*Corresponding authors. *E-mail addresses: wwsun@niglas.ac.cn; jishen@niglas.ac.cn*

ABSTRACT

Understanding the changes in monsoon intensity and ecosystem response at different timescales is crucial for the well-being of humans, yet the paleoclimatic interpretation of stable carbon isotope ($\delta^{13}C$) values from northeast China records is debatable. In this study, reported $\delta^{13}C$ data from 76 surface soils in northeast China are compiled, and a $\delta^{13}C$ record of pyrogenic carbon ($\delta^{13}C_{PyC}$) from Lake Xingkai in northeast

China since the last interglacial period is presented. The aim was to investigate the orbital timescale environmental implication of geological $\delta^{13}C_{PyC}$ data for northeast China. The results showed a distinct increase in $\delta^{13}C$ values of surface soils, which correlated with increasing temperature of the warmest month. Higher temperature favored the expansion of C_4 plants, while precipitation had only a weak correlation with $\delta^{13}C$ values of surface soils in the region. On an orbital timescale, the $\delta^{13}C_{PyC}$ record from Lake Xingkai generally reflected paleovegetation change, suggesting that the abundance of C_4 plants was relatively high during the warm periods, changing to almost purely C_3 plants during the cold periods. Both modern and geological analyses suggest that the climatic factor determining the $\delta^{13}C$ in northeast China was temperature of the warmest month. This is similar to the situation for mid-latitudes such as the Chinese Loess Plateau, in contrast to low latitudes such as southern China.

Keywords: Asian summer monsoon; stable carbon isotopes; C_3/C_4 plants; pyrogenic carbon; lacustrine sediments

1. Introduction

The Asian summer monsoon is an important component of the global climate system that transports heat and moisture from the warmest part of the tropical ocean to higher latitudes, playing a significant role in the socio-economic and agricultural development over a densely populated region (An et al., 2000). Northeast China is in the current East Asian summer monsoon (EASM) margin and particularly sensitive to monsoon variation. However, there remain conflicting interpretations regarding the variation in monsoonal precipitation on decadal to orbital timescales for the region. For example, a large number of stable carbon isotope ($\delta^{13}C$) records from this sensitive zone have been developed to reconstruct the centennial to millennial abrupt monsoon change events since the last deglaciation (Hong et al., 2005; Hong et al., 2010; Chu et al., 2014; Sun et al., 2016). These records show more negative $\delta^{13}C$ values during cold conditions, suggesting that the abrupt changes in monsoon intensity are closely linked to the climatic anomalies in the Northern Hemisphere at high latitude. However, some pollen and sedimentary records from northeast China suggest that the EASM was weakened in response to the cold climate conditions at the high latitudes (Stebich et al., 2009; Xiao et al., 2009; Chen et al., 2015a). Therefore, it is important to clarify these inconsistent interpretations of paleo-records from northeast China.

The $\delta^{13}C$ data from organic matter (OM) derived from terrigenous higher plants have been widely used for paleoenvironmental and paleoclimatic reconstruction in the Asian summer monsoon region in the past two decades (Zhang et al., 2003; Vidic and Montañez, 2004; An et al., 2005; Liu et al., 2005; Zhou et al., 2012; Jia et al., 2015; Yang et al., 2015; Zhang et al., 2015; Rao et al., 2016). However, there is a lack of consistent regional climatic significance of the $\delta^{13}C$ data, examples being that surface soil $\delta^{13}C$ values correlate positively with precipitation in the central of Chinese Loess Plateau, but the correlation is the opposite of that in the sand fields of northern China and Mongolia (An et al., 2005; Feng et al., 2008; Lu et al., 2012; Chen et al., 2015b). In addition, the climatic factor that controls the modern $\delta^{13}C$ values in northeast China has not been well investigated despite its important geographic location.

Pyrogenic carbon (PyC) represents a wide spectrum of carbon-rich material produced either naturally or anthropogenically by combustion or pyrolysis, including partly charred biomass, charcoal, carbonaceous spherules, soot and microcrystalline graphite (Masiello, 2004; Bird and Ascough, 2012). Slightly charred biomass with low aromaticity and high reactivity is formed at low temperature, whereas particulate black carbon with high aromaticity and low reactivity is condensed at high temperature (Bird and Ascough, 2012). The $\delta^{13}C$ values of PyC ($\delta^{13}C_{PyC}$) is unlikely to be subject to significant alteration during pyrolysis, so is likely to record the original $\delta^{13}C$ characteristics of the combusted biomass (Bird and Ascough, 2012; Liu et al., 2013; Wang et al., 2013b). It has been widely used as a proxy to reconstruct paleovegetation and palaeoclimate in southern China (Jia et al., 2003; Zhou et al., 2014, 2017; Sun et al., 2015; Zhang et al., 2015; Sun et al., 2017). In order to clarify the environmental implications of geological $\delta^{13}C_{PyC}$ data for northeast China, we have compiled reported $\delta^{13}C$ values of top soil OM from northeast China under different environments (Rao et al., 2008, 2017; Lu et al., 2012; Chen et al., 2015b; Jia et al., 2016). We then present a $\delta^{13}C_{PyC}$ record from Lake Xingkai in northeast China, covering the last interglacial period and compared the record with a range of other $\delta^{13}C$ records from the Asian summer monsoon region on an orbital timescale.

2. Study region

Northeast China (115°E to 135°E and 38°N to 53°N, Fig. 1a and b) is characterized by plains and sand fields separated by three major mountain systems: The Great Khingan Mountains, the Lesser Khingan Mountains and the Changbai Mountains. The western part is covered mainly by the Hulun Buir sand field and Otindag sand field, and the south-central part and the northeast corner comprise Songnen/Liaohe Plain and Sanjiang Plain, respectively. The climate is influenced by both the EASM and the polar climate system, with a semi-humid to arid pattern. During the winters, the cold and dry northwesterly airflows generated by the Mongolian High prevail in the study region, while during the summers, the warm and moist southerly air masses driven by the pressure gradient between the northwest Pacific and the Eurasian continent interact with cold air from the northwest and produce most of the annual precipitation. The mean annual temperature (MAT) ranges from -4.7 to 10.7 °C and the mean summer temperature ranges from 14.7 to 23.8 °C. Mean annual precipitation (MAP) decreases from the southeast (1000 mm) to the northwest (ca. 150 mm), 80% of which falls in the period of May to September. The vegetation in northeast China is characterized by arid to semi-arid grassland and shrubs in the sand fields, the plains being covered by mixed C_3 and C_4 plants and temperate mixed forest dominated by C_3 plants prevailing in the mountain regions (Qian et al., 2003). Most of the C_4 plants in northeast China belong to the Poaceae, Cyperaceae, Amaranthaceae and Chenopodiaceae; the habitats are dry steppe and saline grassland (Yin and Wang, 1997).

Lake Xingkai (44°32″- 45°21″N, 131°58″- 132°51″E, 65 m above sea level, Fig. 1c) is in a graben basin that formed in the Cenozoic (Wan and Zhong, 1997). It is the largest freshwater lake in northeastern Asia, with a surface area of 4190 km^2 and a maximum water depth of 10 m. It has a catchment of 16,890 km^2 and is fed mainly by five rivers. It has only one outflowing river (the Songacha River) in the northeast, which flows into the Ussuri River (Fig. 1c). The meteorological records from the adjacent Jixi meteorological station (ca.120 km east of the lake) indicate a MAT of 3 °C, a maximum monthly mean temperature of 21 °C in July and a minimum monthly mean temperature of -18 °C in January. The MAP is ca. 540 mm. The modern natural vegetation of the lake catchment is categorized as temperate mixed forest. However, there is a strong altitudinal zonation of vegetation in the region: the landscape is occupied by helophytes, composed primarily of *Alnus sibirica*, *Salix brachypoda*, *Betula fruticosa*, *Spiraea salicifolia*, *Phragmites communis*, *Carex appendiculata*, *Carex lasiacarpa and Carex pseudocuraica* below ca. 200 m, while in the mountainous region, the vegetation is dominated by broadleaved forest and *Pinus koraieusis* forest.

3. Material and methods

3.1. $\delta^{13}C$ data for topsoil and climatic data

All the $\delta^{13}C$ data for topsoil samples were obtained directly from the publications or from the related supplementary information (Fig. 1b). The samples were collected at a depth of ca. 2,- 4 cm, where there was no significant disturbance from human activity. The climate variables for each sampling site were estimated from WorldClim version 2 (http://worldclim.org/version2), which provides gridded climate data at a spatial resolution of 1 km × 1 km. To identify the relationship between $\delta^{13}C$ data of topsoil and climate, we used MAT, MAP, mean temperature and precipitation for the growing season (May to October).

3.2. Coring and dating

In summer of 2008, two parallel and overlapping sediment cores (XK08-A1 and XK08-A2) were collected at a water depth of 7 m near the China-Russia boundary (Fig. 1c, 45°12′21"N, 132°30′33" E) using a UWITEC piston corer. In the laboratory, core correlation between XK08-A1 (308 cm) and XK08-A2 (336 cm) was carried out using surface scanning magnetic susceptibility. Core XK08-A1 was split under subdued red light in the dark room and sectioned at 5-10 cm intervals for optically stimulated luminescence dating. Core XK08-A2 was split into two halves and optically described in the field. The cores were composed mainly of fine-grained, grayish, minerogenic, organic-poor sediments. One half of XK08-A2 was used here and sectioned at 1 cm intervals, and the samples were stored at 4 °C in the repository prior to analysis. Its chronology is based on the correlation of the magnetic susceptibility with XK08-A1, which was dated using the OSL method (Fig. 2a, Long et al., 2015; Sun et al., 2018). It was supported by an AMS ^{14}C age from twigs at 64 cm depth, which was dated to ca. 26.5 cal ka BP in Beta Analytic Inc., Miami, USA. The age-depth model for the upper 70-cm of Lake Xingkai sediment is produced by

Bacon software (Fig. 2b).

3.3 Extraction of pyrogenic carbon and analysis of $\delta^{13}C_{PyC}$

Samples at 1 cm intervals above 70 cm depth and 4 cm intervals below this were used for the analysis of $\delta^{13}C_{PyC}$, yielding a total of 136 samples. Due to that continuum contaiings slightly charred biomass at low temperature, the PyC in the bulk sediment was extracted using the dichromate oxidation method of Lim and Cachier (1996): Freeze-dried bulk sample (ca. 1.0 g) was weighed and treated with HCl (3mol/l); a mixed solution of 3 mol/l HCl and 22 mol/l HF (1: 2, v/v), and HCl (10 mol/l) was added to remove carbonate and part of the silicate fraction. The acid-treated sample was then oxidized using a mixture of $K_2Cr_2O_7$ (0.2 mol/l) and H_2SO_4 (2 mol/l) at 55 °C for 60 h to remove soluble OM and kerogen, the residual refractory carbon being regarded as PyC. The dried sample was then crushed to powder using an agate mortar. The $\delta^{13}C_{PyC}$ value was determined using a Thermo Delta Plus mass spectrometer coupled to an elemental analyzer (Flash EA 1112) at the Nanjing Institute of Geography and Limnology, Chinese Academy of Sciences. The carbon isotope results are expressed in conventional delta notation, as per mil (‰) deviation from the Vienna Peedee Belemnite (VPDB) standard. The calibration and assessment of the reproducibility and accuracy of the isotopic analyses were based on replicate analyses of external working standard materials, and the precision was better than 0.2‰.

4. Results

The $\delta^{13}C$ values ranged from -27.7 to -19.1‰ with a mean of -23.9‰. Regression analysis showed that there was a significant and moderate correlation of $\delta^{13}C$ values with MAT and temperature of the warmest season (Fig. 3a and b, y = 0.261 x – 24.345, $r^2 = 0.28$, $p < 0.001$ and y = 0.422 x- 32.586, $r^2 = 0.30$, $p < 0.001$, respectively), and a significant negative correlation between the topsoil $\delta^{13}C$ values and MAP and growing season precipitation (Fig. 3c and d, y = -0.004 x – 22.124, r^2 = 0.07, $p < 0.05$ and y = -0.004 x – 22.096, $r^2 = 0.06$, $p < 0.05$). The results show clearly that the relationship between topsoil $\delta^{13}C$ values and temperature is stronger than the relationship with precipitation.

As shown in Fig. 4a, the $\delta^{13}C_{PyC}$ values from the lake exhibited wide variation from -29.1 to -21.7‰, with a mean of -24.4‰ along the 336 cm profile. On the basis of the correlated age with OSL dating, the sequence could be divided into three stages: the $\delta^{13}C_{PyC}$ values tended to be more positive in the interglacial stages (MIS 5 and 1) than the last glacial period (MIS 4 to 2). During the last interglacial period, $\delta^{13}C_{PyC}$ values ranged from -24.8 to -21.7‰, with a mean of -23.3‰. During the last glacial period, they decreased significantly during MIS 4 and early MIS 3, ranging from -27.1 to -23.9‰, with a mean of -24.9‰, while they ranged from -29.1 to -24.0‰ also with a mean of -24.9‰, during MIS 2. During the Holocene, the values fluctuated frequently, ranging from -28.6 to -22.0‰, with a mean of -24.1‰.

5. Discussion

5.1. Climatic influence on $\delta^{13}C$ composition of topsoil OM

At a given location, $\delta^{13}C$ values for topsoil samples inherited mainly the overlying vegetation isotopic signature, and were potentially affected by the early decomposition of OM. Generally speaking, terrestrial higher plants can be classified into two principal functional forms: Calvin-Benson (C_3 plants) and Hatch-Slack (C_4 plants), according to the carbon fixation pathway in the process of photosynthesis (Farquhar et al., 1989). The $\delta^{13}C$ values of plants using the C_3 pathway, such as all trees and most shrubs, range from -37‰ to -20‰, with a mean of -27‰, omitting the samples in low-light tropical forest under modern atmospheric CO_2 conditions (Farquhar et al., 1989; Kohn, 2010). C_4 plants, including most warm season grasses/sedges have, however, higher $\delta^{13}C$ values in the range -16‰ to -10‰, with a mean of -13‰ (Farquhar et al., 1989). Similar values were reported in north China, with -26.7‰ for C_3 plants and -12.8‰ for C_4 plants in the Chinese Loess Plateau (Wang et al., 2008); and with -27.8± 1.4‰ for C_3 plants and -13.5± 1.9‰ for C_4 plants in the region with 400 mm isoline of mean annual precipitation (Wang et al., 2013). Field and laboratory investigations suggested that ^{13}C enrichment would occur during decomposition of the plant residue in soil, with a magnitude of 1- 3‰ (Connin et al., 2001; Wang et al., 2008). In this study, the mean $\delta^{13}C$ values of the topsoil OM is about -24‰, with the potentially carbon isotopic fractionation when plant residue decomposes in soil, suggesting a predominance of C_3 plants and low abundance of C_4 plants in northeast China.

The abundance of C_3 and C_4 plants can be estimated by applying the following isotope mass balance equations, using the $\delta^{13}C$ values of the topsoil OM proposed by Wang et al. (2008):

$$\delta^{13}C = \delta^{13}C_{C4} \times C_4\% + \delta^{13}C_{C3} \times (100\% - C_4\%) + 1.8 \quad (1)$$

$$C_4\% = (\delta^{13}C - 1.8 - \delta^{13}C_{C3}) / (\delta^{13}C_{C4} - \delta^{13}C_{C3}) \times 100 \quad (2)$$

where $\delta^{13}C_{C3}$ is the global mean value of $\delta^{13}C$ for C_3 plants, $\delta^{13}C_{C4}$ the end member value of $\delta^{13}C$ for C_4 plants, $\delta^{13}C$ the measured $\delta^{13}C$ value of OM in topsoil and 1.8 the mean value for carbon isotope fraction during decomposition of OM; $C_4\%$ is the relative abundance of C_4 plants, and $100\%- C_4\%$ is the relative abundance of C_3 plants. The estimated relative abundance of C_4 plants in northeast China ranges from 0 to 43.6%, with a mean of 11.0%. The result is consistent with the study of modern C_4 biomass in northeast China, which showed that C_4 plants contributed almost 40% of the total biomass in the dry grassland communities and are rare in the alpine forest (Han et al., 2006). Therefore, soil OM preserves the large isotopic contrast in C_3/C_4 plants, despite minor fractionation between topsoil and the corresponding overlying vegetation.

Temperature and precipitation are the most important climatic factors that can affect the carbon isotopic fractionation during the photosynthetic processes of both C_3 and C_4 plants. More negative $\delta^{13}C$ values of C_3 plants normally occur under relatively humid conditions, resulting from the relatively high stomatal conductance of C_3 plants, therefore increasing intercellular partial pressure of CO_2 under such conditions

(Farquhar et al., 1989). Globally, the $\delta^{13}C$ values of C_3 plants generally decrease with increasing MAP (-0.2‰/ 100 mm), while C_4 plants show a weak positive relationship with MAP (only 0.06‰/ 100 mm). However, the coefficient is largely dependent on plant species (Rao et al., 2017). Wang et al. (2008) measured the $\delta^{13}C$ values of hundreds of C_3 species in north China and found that the value decreased 0.4‰ for every 100 mm increase in MAP. In this study, the $\delta^{13}C$ value of topsoil OM in northeast China also decreases 0.4‰ for every 100 mm increase in MAP; however, that is insignificant. Furthermore, studies of C_3 plants showed mostly negative correlations between $\delta^{13}C$ values and MAT, without controlling MAP (Rao et al., 2017). After correction for the effect of MAP, temperature exerts only a minimal effect on $\delta^{13}C$ values of C_3 plants, with 0.1‰/°C in north China (Diefendorf et al., 2010; Wang et al., 2013). Therefore, the effect of the main climatic factors on $\delta^{13}C$ values of pure C_3 plants could not explain the relationship between $\delta^{13}C$ values of topsoil OM and temperature and precipitation in northeast China.

The significant positive correlation between temperature and the $\delta^{13}C$ values of topsoil samples is consistent with studies of the regions with mixed C_3/C_4 vegetation or pure C_4 vegetation, such as the Chinese Loess Plateau (An et al., 2005; Rao et al., 2017). However, the weak negative correlation between precipitation and $\delta^{13}C$ values of topsoil samples in northeast China contrasts with the significant negative correlation between rainfall and the $\delta^{13}C$ values of topsoil samples in the low latitudes (Rao et al., 2010 and 2017). There is a general agreement that C_4 plants are more competitive than C_3 plants in a warm and dry environment (Farquhar et al., 1989;

Sage et al., 1999); however, higher water use efficiency of C_4 plants than C_3 plants cannot explain the weak negative correlation between precipitation and the $\delta^{13}C$ values of topsoil samples. One of the alternative interpretations is that the growth of C_4 plants can be limited in regions with a cold climate (Sage et al., 1999). Globally, only 3 to 5 modern C_4 species are found in the region above 60 °N and the most typical C_4 vegetation is distributed in relatively hot and dry areas in the low latitudes (Sage et al., 1999). Investigations of C_4 plants in the Qinghai-Tibetan Plateau also demonstrated that very few C_4 species exist in the high altitude regions (Wang et al., 2004; Li et al., 2009). Laboratory data also indicate a close correlation between the distribution of C_4 plants and growing season temperature, and C_4 photosynthesis is inhibited in regions where the mean growing season temperature is < 16 °C under modern atmospheric CO_2 conditions (McWilliam and Naylor, 1967). The summer temperature in northeast China ranges from 14.7 to 23.8 °C, above the threshold temperature of 16 °C on average. This possibly explains the minor contribution of C_4 plants in this region, and the abundance of C_4 plants positively correlated with the temperature of the warmest month temperature. In addition, different carbon isotope fractionation response of C_3 and C_4 plants to precipitation may also weaken the correlation between rainfall and the $\delta^{13}C$ values of topsoil samples in northeast China.

5.2. Variation in relative abundance of C_3/C_4 plants in the late Quaternary

In natural burns and controlled field burns, the carbon isotope fractionation of PyC from C_3 plant combustion varies from -3 to 3‰ with a mean of -0.3± 1.0‰, while the fractionation for PyC from C_4 plants combustion ranges from -10 to 3‰

with a mean of -1.7± 2.4‰ (Wang et al., 2013b). This may be attributed to differences in the proportion of isotopically distinct volatile and refractory compounds between plants and pyrolysis temperature, and the more negative fractionation for PyC from C_4 plants may result from the more depleted carbon being protected in phytoliths (Krull et al., 2003; Das et al., 2010; Bird and Ascough, 2012). In general, biochemical fractions of plant material such as lignin, cellulose and lipids are depleted in ^{13}C compared with the whole plant, while hemicellulose, sugars, amino acids and pectin are enriched in ^{13}C (Deines, 1980). For example, monosaccharides were generally enriched in ^{13}C by 1 to 16‰ compared with lipids within single organisms (Van Dongen et al., 2002). Thus, the preferential loss of ^{13}C-enriched biochemical fractions of plants during biomass burning might result in depletion of ^{13}C in the PyC (Das et al., 2010). Some recent work showed that waxes and other paraffinic components can survive dichromate oxidation, suggesting that the method might not have completely removed organics (Knicker et al., 2007; Ascough et al., 2008). However, this might also be a result of the refractory compounds retained within the charcoal structure due to incomplete burning. Although the carbon isotope fractionation of plants during pyrolysis is variable, $\delta^{13}C_{PyC}$ and $\delta^{13}C$ values of the bulk soil OM is strongly positive and the difference between them is also within the small range -1.5 to 1.3‰ in the Chinese Loess Plateau (Liu et al., 2013). Therefore, $\delta^{13}C_{PyC}$ may generally reflect $\delta^{13}C$ of paleovegetation change at a given locality.

On an orbital timescale, large changes in temperature, precipitation, pCO_2 level and $\delta^{13}C$ value of atmospheric CO_2 may directly influence the $\delta^{13}C$ values of plant tissues. The $\delta^{13}C$ values of C_3 plants might increase with increasing temperature (ca. 0.1‰/ °C) and decrease with increasing precipitation (ca. 0.4‰/ 100 mm) in northern China (Wang et al., 2013a). However, after correction of both temperature and precipitation, climate exerts a negligible effect on the $\delta^{13}C$ values of C_3 plants (Wang et al., 2013; Yang et al., 2015). Due to the lack of long term quantitative climatic data for northeast China, we suggest that the effect of the response of $\delta^{13}C$ values of plants to different climatic conditions is also insignificant in this study. During the last 130 ka, pCO_2 level in the interglacial periods was ca. 80 ppmv higher than in the last glacial period, and pCO_2 has increased by 70 ppmv since the industrial revolution (Fig. 4e, Friedli et al., 1986; Monnin, 2001, 2004). Although some studies suggested a significant negative relationship between pCO_2 and $\delta^{13}C$ of C_3 plants (Feng et al., 1995; Schubert and Jahren, 2012), the estimated depletion of $\delta^{13}C$ values of C_3 plants is close to the $\delta^{13}C$ value of atmospheric CO_2, which has decreased during the last two centuries due to fossil combustion and vegetation destruction (Friedli et al., 1986; Keeling et al., 2017). Therefore, we ignored the effect of changes in pCO_2 on the $\delta^{13}C$ value of C_3 plants. The $\delta^{13}C$ value of atmospheric CO_2 has decreased to -8.4‰ recently, which is about 2.0‰ lower than that during the pre-industrial period (Keeling et al., 2017). Hence, the mean $\delta^{13}C$ value of C_3 and C_4 plants would increase by 2.0‰ during the period before the industrial revolution. The $\delta^{13}C$ value of atmospheric CO_2 and fractionation during pyrolysis, the $\delta^{13}C$ value of PyC derived from C_3 would become -25.3± 1.7‰, while the corrected $\delta^{13}C$ value for PyC derived from C_4 plants is -12.7± 3.1‰. Therefore, the abundance of C_3 and C_4 plants can be estimated by the modified equation using the $\delta^{13}C_{PyC}$ values:

$$C_4\% = (\delta^{13}C_{PyC} - \delta^{13}C_{PyC\text{-}C3}) / (\delta^{13}C_{PyC\text{-}C4} - \delta^{13}C_{PyC\text{-}C3}) \times 100 \quad (3)$$

where $\delta^{13}C_{PyC\text{-}C3}$ is the end member value of $\delta^{13}C$ for PyC derived from C_3 plants, $\delta^{13}C_{PyC\text{-}C4}$ the end member value of $\delta^{13}C$ for PyC derived from C_4 plants and $\delta^{13}C_{PyC}$ the measured $\delta^{13}C$ value of PyC in Lake Xingkai sediment.

The estimated change in the relative abundance of C_4 plants since the last interglacial period is shown in Fig. 4b. The long term trend suggests a C_4 plant expansion during warm periods and purely C_3 plants during cold periods. During the last interglacial period, the relative abundance of C_4 plants ranged from 3.8 to 28.7% with a mean of 16.3%, suggesting a mixed C_3/C_4 plant ecosystem but dominated by C_3 plants in and around the catchment of Lake Xingkai. During the last glacial period, the mean $\delta^{13}C_{PyC}$ values were nearly same as $\delta^{13}C_{PyC\text{-}C3}$, indicating that the land was nearly covered by pure C_3 plants, with only about 4.8% C_4 plants. During the Holocene, C_4 plants reappeared with an abundance up to 26.3% and a mean of 11.7%. The accuracy of the estimates could also be influenced by the uncertainty in the $\delta^{13}C$ values of both C_3 and C_4 plants during the pyrolysis process. However, our estimate of the C_4 plant abundance during the interglacial periods is close to the modern abundance in the plains and grasslands in northeast China (Han et al., 2006).

5.3. Regional comparison of C_3/C_4 plant evolution

The increase in the relative abundance of C_4 plants from northeast China since the last glacial maximum is consistent with the record of compound-specific carbon isotope composition of long chain *n*-alkanes ($\delta^{13}C_{n\text{-alkanes}}$) from Huola Basin and Wudalianchi in Songnen Plain. These data show that the *n*-alkanes were more ^{13}C depleted during the late glacial period (Fig. 5b, Wei et al., 2015; Wang et al., 2017). Similarly, the record of $\delta^{13}C_{n\text{-alkanes}}$ from the Sea of Japan also shows that *n*-alkanes are depleted in ^{13}C by ca. 1‰ in colder climates than in a warmer climate (Yamada and Ishiwatari, 1999). In the Chinese Loess Plateau, the relative abundance of C_3 and C_4 plants has been extensively investigated using $\delta^{13}C_{n\text{-alkanes}}$ or $\delta^{13}C$ of bulk OM from the loess-paleosol profiles during the last decades (Fig. 5c, Zhang et al., 2003; Vidic and Montañez, 2004; Liu et al., 2005; Yang et al., 2015). These records show that the $\delta^{13}C$ values along a temporal sequence were more positive in paleosol layers and more negative in loess layers. Along a spatial gradient, the estimated relative abundance of C_4 plants increased from < 5% in the northwest to 10-20% in the southeast during the last glacial maximum. During the mid-Holocene, the estimated relative abundance of C_4 plants increased from 10% to 20% in the northwest to > 40% in the southeast (Yang et al., 2015). However, in the low latitudes of the Asian summer monsoon regions, decreases in the relative abundance of C_4 plants from the last glacial maximum to the Holocene were recorded by way of the $\delta^{13}C_{PyC}$ record from lacustrine sediments in southwest China (Fig. 5d, Zhang et al., 2015), agreeing well with the $\delta^{13}C_{n\text{-alkanes}}$ records from the northern Bay of Bengal and the northern South China Sea (Fig. 5e and f, Zhou et al., 2012; Contreras-Rosales et al., 2014). The different glacial-interglacial vegetation changes between the mid and low latitudes can be attributed mainly to a different response of C_4 plants to the regional climate change instead of global pCO_2 (Huang et al., 2001; Rao et al., 2017).

As discussed above, growing season temperature might be the dominant factor controlling the distribution and relative abundance of C_4 plants in mid latitudes (Rao et al., 2017). During the last glacial maximum, pollen records for south China suggest that the temperature was 2- 3 °C lower than at present (Wang et al., 2012; Chen et al., 2014), while the reconstructed summer air temperature based on gastropods, pedogenic carbonate, phytoliths and fossil branched tetraether membrane lipids of soil bacteria from the Chinese Loess Plateau suggest a 6- 7 °C cooling in the summer (Fig. 4d, Lu et al., 2007; Eagle et al., 2013; Peterse et al., 2014). The magnitude and pattern of cooling during the late glacial period is in agreement with the paleoclimate modeling, suggesting in the Northern Hemisphere, 5- 10 °C cooling in the mid high latitudes, and 2- 5 °C cooling in the tropical continent and the ocean (Braconnot et al., 2007). Therefore, we infer that the growing season temperature might be lower than the threshold temperature in northeast China, but still high enough for the growth of C_4 plants at low latitudes. During the last glacial period, the weakened Asian summer monsoon and lower temperature led to a southward shift of C_4 plants, and their general disappearance from northeast China. In contrast, in the low latitudes, weakened Asian summer monsoon and low pCO_2 were favorable for the expansion of C_4 plants during the last glacial maximum, and the vegetation composition in the Holocene (dominated by C_3 plants) was driven mainly by the strengthening of the Asian summer monsoon (Fig. 5d to f, Zhou et al., 2012; Contreras-Rosales et al., 2014;

Zhang et al., 2015).

6. Conclusions

We compiled reported $\delta^{13}C$ values for topsoil OM from northeast China and presented a $\delta^{13}C_{PyC}$ record from Lake Xingkai in northeast Asia since the last interglacial period in order to investigate the environmental implication of geological $\delta^{13}C_{PyC}$ data for northeast China. The results show that warmest month temperature is the dominant climatic factor determining the $\delta^{13}C$ values of surface soil, with higher temperature favoring the expansion of C_4 plants, while precipitation had only a weak correlation with $\delta^{13}C$ values of surface soils in northeast China. On an orbital timescale, the $\delta^{13}C_{PyC}$ record from Lake Xingkai suggests that the abundance of C_4 plants was relatively high during warm periods and ranged to almost purely C_3 plants during cold periods. Both modern and geological analysis suggest that the climatic implication of $\delta^{13}C$ of OM derived from terrestrial higher plants in northeast China is similar to that of the Chinese Loess Plateau, in contrast to that for low latitudes.

Acknowledgments

We would like to express our gratitude to B. Zhou and and two anonymous reviewers for their helpful comments. We would also like to express our gratitude to Y. Wang for field assistance. The research was supported by the National Natural Science Foundation of China (Grants. 41430530, 41621002 and 41702183) and the

National Key R&D Program of China (Grant 2017YFA0605203).

References

An, Z., Huang, Y., Liu, W., Guo, Z., Steven, C., Li, L., Warren, P., Ning, Y., Cai, Y., Zhou, W., Lin, B., Zhang, Q., Cao, Y., Qiang, X., Chang, H., Wu, Z., 2005. Multiple expansions of C_4 plant biomass in East Asia since 7 Ma coupled with strengthened monsoon circulation. Geology 33, 705-708.

An, Z., Porter, S.C., Kutzbach, J.E., Wu, X., Wang, S., Liu, X., Li, X., Zhou, W., 2000. Asynchronous Holocene optimum of the East Asian monsoon. Quaternary Science Reviews 19, 743-762.

Ascough, P.L., Bird, M.I., Wormald, P., Snape, C.E., Apperley, D., 2008. Influence of production variables and starting material on charcoal stable isotopic and molecular characteristics. Geochimica et Cosmochimica Acta 72, 6090-6102.

Bird, M.I., Ascough, P.L., 2012. Isotopes in pyrogenic carbon: A review. Organic Geochemistry 42, 1529-1539.

Braconnot, P., Otto-Bliesner, B., Harrison, S., Joussaume, S., Peterchmitt, J.Y., Abe-Ouchi, A., Crucifix, M., Driesschaert, E., Fichefet, T., Hewitt, C.D., Kageyama, M., Kitoh, A., Laîné, A., Loutre, M.F., Marti, O., Merkel, U., Ramstein, G., Valdes, P., Weber, S.L., Yu, Y., Zhao, Y., 2007. Results of PMIP2 coupled simulations of the Mid-Holocene and Last Glacial Maximum - Part 1: experiments and large-scale features. Climate of the Past 3, 261-277.

Chen, R., Shen, J., Li, C., Zhang, E., Sun, W., Ji, M., 2015a. Mid- to late-Holocene East Asian summer monsoon variability recorded in lacustrine sediments from Jingpo Lake, Northeastern China. The Holocene 25, 454-468.

Chen, X., Chen, F., Zhou, A., Huang, X., Tang, L., Wu, D., Zhang, X., Yu, J., 2014. Vegetation history, climatic changes and Indian summer monsoon evolution during the Last Glaciation (36,400–13,400 cal yr BP) documented by sediments from Xingyun Lake, Yunnan, China. Palaeogeography, Palaeoclimatology, Palaeoecology 410, 179-189.

Chen, Y.Y., Lu, H.Y., Zhang, E.L., Zhang, H.Y., Xu, Z.W., Yi, S.W., Wu, S.Y., 2015b. Test stable carbon isotopic composition of soil organic matters as a proxy indicator of past precipitation: Study of the sand fields in northern China. Quaternary International 372, 79-86.

Chu, G., Sun, Q., Xie, M., Lin, Y., Shang, W., Zhu, Q., Shan, Y., Xu, D., Rioual, P., Wang, L., Liu, J., 2014. Holocene cyclic climatic variations and the role of the Pacific Ocean as recorded in varved sediments from northeastern China. Quaternary Science Reviews 102, 85-95.

Connin, S.L., Feng, X., Virginia, R.A., 2001. Isotopic discrimination during long-term decomposition in an arid land ecosystem. Soil Biology and Biochemistry 33, 41-51.

Contreras-Rosales, L.A., Jennerjahn, T., Tharammal, T., Meyer, V., Lückge, A., Paul, A., Schefuß, E., 2014. Evolution of the Indian Summer Monsoon and terrestrial vegetation in the Bengal region during the past 18 ka. Quaternary Science Reviews 102, 133-148.

Das, O., Wang, Y., Hsieh, Y.-P., 2010. Chemical and carbon isotopic characteristics of ash and smoke derived from burning of C_3 and C_4 grasses. Organic Geochemistry, 41, 263-269.

Deines, P., 1980. The isotopic composition of reduced organic carbon. In: Fontes, P.F.C. (Ed.), The Terrestrial Environment. Elsevier, Amsterdam, pp. 329-406.

Diefendorf, A.F., Mueller, K.E., Wing, S.L., Koch, P.L., Freeman, K.H., 2010. Global patterns in leaf ^{13}C discrimination and implications for studies of past and future climate. Proceedings of the National Academy of Sciences 107, 5738-5743.

Eagle, R.A., Risi, C., Mitchell, J.L., Eiler, J.M., Seibt, U., Neelin, J.D., Li, G., Tripati, A.K., 2013. High regional climate sensitivity over continental China constrained by glacial-recent changes in temperature and the hydrological cycle. Proceedings of the National Academy of Sciences 110, 8813-8818.

Farquhar, G.D., Ehleringer, J.R.A., T, H., 1989. Carbon isotope discrimination and photosynthesis. Annual Review of Plant Physiology and Plant Molecular Biology 40, 503-537.

Feng, X., Epstein, S., 1995. Carbon isotopes of trees from arid environments and implications for reconstructing atmospheric CO_2 concentration. Geochimica et Cosmochimica Acta 59, 2599-2608.

Feng, Z.D., Wang, L.X., Ji, Y.H., Guo, L.L., Lee, X.Q., Dworkin, S.I., 2008. Climatic dependency of soil organic carbon isotopic composition along the S–N Transect from 34°N to 52°N in central-east Asia. Palaeogeography, Palaeoclimatology, Palaeoecology 257, 335-343.

Friedli, H., Lotscher, H., Oeschger, H., Siegenthaler, U., Stauffer, B., 1986. Ice core record of the $^{13}C/^{12}C$ ratio of atmospheric CO_2 in the past two centuries. Nature 324, 237-238.

Han, M., Yang, L., Zhang, Y., Zhou, G., 2006. The biomass of C_3 and C_4 plant function groups in *Leymus chinensis* communities and their response to environmental change along Northeast China transect. Acta Ecological Sinica 26, 1825-1832 (in Chinese).

Hong, B., Hong, Y.T., Lin, Q.H., Shibata, Y., Uchida, M., Zhu, Y.X., Leng, X.T., Wang, Y., Cai, C.C., 2010. Anti-phase oscillation of Asian monsoons during the Younger Dryas period: Evidence from peat cellulose $\delta^{13}C$ of Hani, Northeast China. Palaeogeography, Palaeoclimatology, Palaeoecology 297, 214-222.

Hong, Y.T., Hong, B., Lin, Q.H., Shibata, Y., Hirota, M., Zhu, Y.X., Leng, X.T., Wang, Y., Wang, H., Yi, L., 2005. Inverse phase oscillations between the East Asian and Indian Ocean summer monsoons during the last 12 000 years and paleo-El Niño.

Earth and Planetary Science Letters 231, 337-346.

Huang, Y., Street-Perrott, F.A., Metcalfe, S.E., Brenner, M., Moreland, M., Freeman, K.H., 2001. Climate change as the dominant control on glacial-interglacial variations in C_3 and C_4 plant abundance. Science 293, 1647-1651.

Jia, G., Bai, Y., Yang, X., Xie, L., Wei, G., Ouyang, T., Chu, G., Liu, Z., Peng, P.a., 2015. Biogeochemical evidence of Holocene East Asian summer and winter monsoon variability from a tropical maar lake in southern China. Quaternary Science Reviews 111, 51-61.

Jia, G., Peng, P.a., Zhao, Q., Jian, Z., 2003. Changes in terrestrial ecosystem since 30 Ma in East Asia: Stable isotope evidence from black carbon in the South China Sea. Geology 31, 1093-1096.

Jia, Y., Wang, G., Tan, Q., Chen, Z., 2016. Temperature exerts no influence on organic matter $\delta^{13}C$ of surface soil along the 400 mm isopleth of mean annual precipitation in China. Biogeosciences 13, 5057-5064.

Jouzel, J., Masson-Delmotte, V., Cattani, O., Dreyfus, G., Falourd, S., Hoffmann, G., Minster, B., Nouet, J., Barnola, J.M., Chappellaz, J., Fischer, H., Gallet, J.C., Johnsen, S., Leuenberger, M., Loulergue, L., Luethi, D., Oerter, H., Parrenin, F., Raisbeck, G., Raynaud, D., Schilt, A., Schwander, J., Selmo, E., Souchez, R., Spahni, R., Stauffer, B., Steffensen, J.P., Stenni, B., Stocker, T.F., Tison, J.L., Werner, M., Wolff, E.W., 2007. Orbital and millennial Antarctic climate variability over the past 800,000 years. Science 317, 793-796.

Keeling, R.F., Graven, H.D., Welp, L.R., Resplandy, L., Bi, J., Piper, S.C., Sun, Y., Bollenbacher, A., Meijer, H.A.J., 2017. Atmospheric evidence for a global secular increase in carbon isotopic discrimination of land photosynthesis. Proceedings of the National Academy of Sciences 114, 10361-10366.

Knicker, H., Müller, P., Hilscher, A., 2007. How useful is chemical oxidation with dichromate for the determination of “Black Carbon” in fire-affected soils?

Geoderma 142, 178-196.

Kohn, M.J., 2010. Carbon isotope compositions of terrestrial C_3 plants as indicators of (paleo)ecology and (paleo)climate. Proceedings of the National Academy of Sciences 107, 19691-19695.

Krull, E.S., Skjemstad, J.O., Graetz, D., Grice, K., Dunning, W., Cook, G., Parr, J.F., 2003. ^{13}C-depleted charcoal from C_4 grasses and the role of occluded carbon in phytoliths. Organic Geochemistry 34, 1337-1352.

Li, J., Wang, G., Liu, X., Han, J., Liu, M., Liu, X., 2009. Variations in carbon isotope ratios of C_3 plants and distribution of C_4 plants along an altitudinal transect on the eastern slope of Mount Gongga. Science in China Series D: Earth Sciences 52, 1714-1723.

Liu, L., Song, Y., Cui, L., Hao, Z., 2013. Stable carbon isotopic composition of black carbon in surface soil as a proxy for reconstructing vegetation on the Chinese Loess Plateau. Palaeogeography, Palaeoclimatology, Palaeoecology 388, 109-114.

Liu, W., Huang, Y., An, Z., Clemens, S.C., Li, L., Prell, W.L., Ning, Y., 2005. Summer monsoon intensity controls C_4/C_3 plant abundance during the last 35 ka in the Chinese Loess Plateau: Carbon isotope evidence from bulk organic matter and individual leaf waxes. Palaeogeography, Palaeoclimatology, Palaeoecology 220, 243-254.

Long, H., Shen, J., Wang, Y., Gao, L., Frechen, M., 2015. High-resolution OSL dating of a late Quaternary sequence from Xingkai Lake (NE Asia): Chronological challenge of the “MIS 3a Mega-paleolake” hypothesis in China. Earth and Planetary Science Letters 428, 281-292.

Lu, H.-Y., Wu, N.-Q., Liu, K.-B., Jiang, H., Liu, T.-S., 2007. Phytoliths as quantitative indicators for the reconstruction of past environmental conditions in China II: palaeoenvironmental reconstruction in the Loess Plateau. Quaternary Science

Reviews 26, 759-772.

Lu, H., Zhou, Y., Liu, W., Mason, J., 2012. Organic stable carbon isotopic composition reveals late Quaternary vegetation changes in the dune fields of northern China. Quaternary Research 77, 433-444.

Luthi, D., Le Floch, M., Bereiter, B., Blunier, T., Barnola, J.-M., Siegenthaler, U., Raynaud, D., Jouzel, J., Fischer, H., Kawamura, K., Stocker, T.F., 2008. High-resolution carbon dioxide concentration record 650,000-800,000 years before present. Nature 453, 379-382.

Marino, B.D., McElroy, M.B., 1991. Isotopic composition of atmospheric CO_2 inferred from carbon in C_4 plant cellulose. Nature 349, 127-131.

Masiello, C.A., 2004. New directions in black carbon organic geochemistry. Marine Chemistry 92, 201-213.

McWilliam, J.R., Naylor, A.W., 1967. Temperature and plant adaptation. I. Interaction of temperature and light in the synthesis of chlorophyll in Corn. Plant Physiology 42, 1711-1715.

Monnin, E., 2001. Atmospheric CO_2 concentrations over the last glacial termination. Science 291, 112-114.

Monnin, E., Steig, E.J., Siegenthaler, U., Kawamura, K., Schwander, J., Stauffer, B., Stocker, T.F., Morse, D.L., Barnola, J.-M., Bellier, B., Raynaud, D., Fischer, H., 2004. Evidence for substantial accumulation rate variability in Antarctica during the Holocene, through synchronization of CO_2 in the Taylor Dome, Dome C and DML ice cores. Earth and Planetary Science Letters 224, 45-54.

Peterse, F., Martínez-García, A., Zhou, B., Beets, C.J., Prins, M.A., Zheng, H., Eglinton, T.I., 2014. Molecular records of continental air temperature and monsoon precipitation variability in East Asia spanning the past 130,000 years. Quaternary Science Reviews 83, 76-82.

Qian, H., Yuan, X.-Y., Chou, Y.-L., 2003. Forest vegetation of Northeast China. In:

Kolbek, J., Šrůtek, M., Box, E.O. (Eds.), Forest Vegetation of Northeast Asia. Springer Netherlands, Dordrecht, pp. 181-230.

Rao, Z., Guo, W., Cao, J., Shi, F., Jiang, H., Li, C., 2017. Relationship between the stable carbon isotopic composition of modern plants and surface soils and climate: A global review. Earth-Science Reviews 165, 110-119.

Rao, Z., Jia, G., Li, Y., Chen, J., Xu, Q., Chen, F., 2016. Asynchronous evolution of the isotopic composition and amount of precipitation in north China during the Holocene revealed by a record of compound-specific carbon and hydrogen isotopes of long-chain *n*-alkanes from an alpine lake. Earth and Planetary Science Letters 446, 68-76.

Rao, Z., Jia, G., Zhu, Z., Wu, Y., Zhang, J., 2008. Comparison of the carbon isotope composition of total organic carbon and long-chain *n*-alkanes from surface soils in eastern China and their significance. Chinese Science Bulletin 53, 3921-3927.

Rao, Z., Zhu, Z., Jia, G., Chen, F., Barton, L., Zhang, J., Qiang, M., 2010. Relationship between climatic conditions and the relative abundance of modern C_3 and C_4 plants in three regions around the North Pacific. Chinese Science Bulletin 55, 1931-1936.

Sage, R.F., Wedin, D.A., Li, M., 1999. The biogeography of C_4 photosynthesis: patterns and controlling factors. In: Sage, R.F., Monson, R.K. (Eds.), C_4 plant Biology. San Diego, California, pp. 313-373.

Schubert, B.A., Jahren, A.H., 2012. The effect of atmospheric CO_2 concentration on carbon isotope fractionation in C_3 land plants. Geochimica et Cosmochimica Acta 96, 29-43.

Stebich, M., Mingram, J., Han, J., Liu, J., 2009. Late Pleistocene spread of (cool-)temperate forests in Northeast China and climate changes synchronous with the North Atlantic region. Global and Planetary Change 65, 56-70.

Sun, Q., Xie, M., Lin, Y., Shan, Y., Zhu, Q., Xu, D., Su, Y., Rioual, P., Chu, G., 2016.

An *n*-alkane and carbon isotope record during the last deglaciation from annually laminated sediment in Lake Xiaolongwan, northeastern China. Journal of Paleolimnology 56, 189-203.

Sun, W., Zhang, E., Jones, R.T., Liu, E., Shen, J., 2015. Asian summer monsoon variability during the late glacial and Holocene inferred from the stable carbon isotope record of black carbon in the sediments of Muge Co, southeastern Tibetan Plateau, China. The Holocene 25, 1857-1868.

Sun, W., Shen, J., Yu, S., Long, H., Zhang, E., Liu, E., Chen, R., 2018. A lacustrine record of East Asian summer monsoon and atmospheric dust loading since the last interglaciation from Lake Xingkai, NE China. Quaternary Research 89, 270-280.

Sun, W., Zhang, E., Liu, E., Ji, M., Chen, R., Zhao, C., Shen, J., Li, Y., 2017. Oscillations in the Indian summer monsoon during the Holocene inferred from a stable isotope record from pyrogenic carbon from Lake Chenghai, southwest China. Journal of Asian Earth Sciences 134, 29-36.

van Dongen, B.E., Schouten, S., Sinninghe Damsté, J.S., 2002. Carbon isotope variability in monosaccharides and lipids of aquatic algae and terrestrial plants. Marine Ecology Progress Series 232, 83-92.

Vidic, N.J., Montañez, I.P., 2004. Climatically driven glacial-interglacial variations in C_3 and C_4 plant proportions on the Chinese Loess Plateau. Geology 32, 337-340.

Wang, G., Feng, X., Han, J., Zhou, L., Tan, W., Su, F., 2008. Paleovegetation reconstruction using $\delta^{13}C$ of soil organic matter. Biogeosciences 5, 1325-1337.

Wang, G., Li, J., Liu, X., Li, X., 2013a. Variations in carbon isotope ratios of plants across a temperature gradient along the 400 mm isoline of mean annual precipitation in north China and their relevance to paleovegetation reconstruction. Quaternary Science Reviews 63, 83-90.

Wang, G., Wang, Y., Wei, Z., Wu, B., Wang, Z., Sun, Z., Xu, L., Wang, Y., 2017.

Climate conditions and relative abundance of C_3 and C_4 vegetation during the past 40 ka inferred from lake sediments in Wudalianchi, northeast China. Journal of Paleolimnology 58, 243-256.

Wang, L., Lü, H., Wu, N., Chu, D., Han, J., Wu, Y., Wu, H., Gu, Z., 2004. Discovery of C_4 species at high altitude in Qinghai-Tibetan Plateau. Chinese Science Bulletin 49, 1392-1396.

Wang, S., Lu, H., Han, J., Chu, G., Liu, J., Negendank, J.F.W., 2012. Palaeovegetation and palaeoclimate in low-latitude southern China during the Last Glacial Maximum. Quaternary International 248, 79-85.

Wang, X., Cui, L., Xiao, J., Ding, Z., 2013b. Stable carbon isotope of black carbon in lake sediments as an indicator of terrestrial environmental changes: An evaluation on paleorecord from Daihai Lake, Inner Mongolia, China. Chemical Geology 347, 123-134.

Wei, Z., Wang, Y., Wu, B., Wang, Z., Wang, G., 2015. Paleovegetation inferred from the carbon isotope composition of long-chain *n*-alkanes in lacustrine sediments from the Song-nen Plain, northeast China. Journal of Paleolimnology 54, 345-358.

Xiao, J., Chang, Z., Wen, R., Zhai, D., Itoh, S., Lomtatidze, Z., 2009. Holocene weak monsoon intervals indicated by low lake levels at Hulun Lake in the monsoonal margin region of northeastern Inner Mongolia, China. The Holocene 19, 899-908.

Yamada, K., Ishiwatari, R., 1999. Carbon isotopic compositions of long-chain *n*-alkanes in the Japan Sea sediments: implications for paleoenvironmental changes over the past 85 kyr. Organic Geochemistry 30, 367-377.

Yang, S., Ding, Z., Li, Y., Wang, X., Jiang, W., Huang, X., 2015. Warming-induced northwestward migration of the East Asian monsoon rain belt from the Last Glacial Maximum to the mid-Holocene. Proceedings of the National Academy of

Sciences 112, 13178-13183.

Zhang, E., Sun, W., Zhao, C., Wang, Y., Xue, B., Shen, J., 2015. Linkages between climate, fire and vegetation in southwest China during the last 18.5 ka based on a sedimentary record of black carbon and its isotopic composition. Palaeogeography, Palaeoclimatology, Palaeoecology 435, 86-94.

Zhang, Z., Zhao, M., Lu, H., Faiia, A.M., 2003. Lower temperature as the main cause of C_4 plant declines during the glacial periods on the Chinese Loess Plateau. Earth and Planetary Science Letters 214, 467-481.

Zhou, B., Bird, M., Zheng, H., Zhang, E., Wurster, C.M., Xie, L., Taylor, D., 2017. New sedimentary evidence reveals a unique history of C_4 biomass in continental East Asia since the early Miocene. Scientific Reports 7, 170.

Zhou, B., Shen, C.D., Sun, W.D., Bird, M., Ma, W.T., Taylor, D., Liu, W.G., Peterse, F., Yi, W.X., Zheng, H.B., 2014. Late Pliocene-Pleistocene expansion of C_4 vegetation in semiarid East Asia linked to increased burning. Geology 42, 1067-1070.

Zhou, B., Zheng, H., Yang, W., Taylor, D., Lu, Y., Wei, G., Li, L., Wang, H., 2012. Climate and vegetation variations since the LGM recorded by biomarkers from a sediment core in the northern South China Sea. Journal of Quaternary Science 27, 948-955.

Fig. 1. (a) Location of Lake Xingkai (1, triangle) and the other paleoclimatic sites (circles) mentioned in Fig. 4. Arrows indicate the dominant atmospheric circulation systems in the region. 2, Wudalianchi in northeast China (Wang et al., 2017); 3, Xifeng profile in the Chinese Loess Plateau (Liu et al., 2005); 4, Lake Tengchongqinghai in southwest China (Zhang et al., 2015); 5, Core MD05-2905 in the South China Sea (Zhou et al., 2012) and 6, Core SO188-342KL in the Bay of

ACCEPTED MANUSCRIPT

Bengal (Contreras-Rosales et al., 2014). (b) Map of study region showing locations of reported $\delta^{13}C$ values of surface soils in northeast China, and (c) location of coring site in Lake Xingkai.

Fig. 2. (a) Stratigraphy correlation of core XK08-A2 (red), XK-1 (blue), and XK08-A1 (purple), dated using the optically stimulated luminescence method (Long et al., 2015; Sun et al., 2018); (b) Age-depth model for the Lake Xingkai upper 70-cm sediment produced with Bacon software. Dotted lines indicate the 95% confidence range and the solid line indicates the weighted mean ages for each depth;

Fig. 3. Linear correlations between $\delta^{13}C$ values of surface soils and (a) corresponding MAT, (b) warmest month temperature, (c) MAP and (d) growing season precipitation.

Fig. 4. Comparison of (a) $\delta^{13}C_{PyC}$ record from Lake Xingkai with other environments. (b) Estimated C_4 plants relative abundance around Lake Xingkai, the standard deviation (σ) is ca. 15%; (c) EASM index derived from core XK08-A2 grain size end members (Sun et al., 2018); (d) MAT inferred from phytoliths at Weinan section in the Chinese Loess Plateau (Lu et al., 2007); (e) Vostok ice core CO_2 concentration (Jouzel et al., 2007; Luthi et al., 2008).

Fig. 5. Latitudinal comparison of C_3/C_4 plants relative abundance change since the last 40 ka. (a) $\delta^{13}C_{PyC}$ record from Lake Xingkai; (b) weighted mean average $\delta^{13}C$ of long chain *n*-alkanes from Wudalianchi in northeast China (Wang et al., 2017); (c) $\delta^{13}C$ of C_{31} *n*-alkane from Xifeng profile in the Chinese Loess Plateau (Liu et al., 2005); (d) $\delta^{13}C_{PyC}$ record from Lake Tengchongqinghai in southwest China (Zhang et al., 2015); weighted mean average $\delta^{13}C$ of specific *n*-alkanes from Core MD05-2905 in the South China Sea (e, Zhou et al., 2012) and Core SO188-342KL in the Bay of

Bengal(f, Contreras-Rosales et al., 2014).

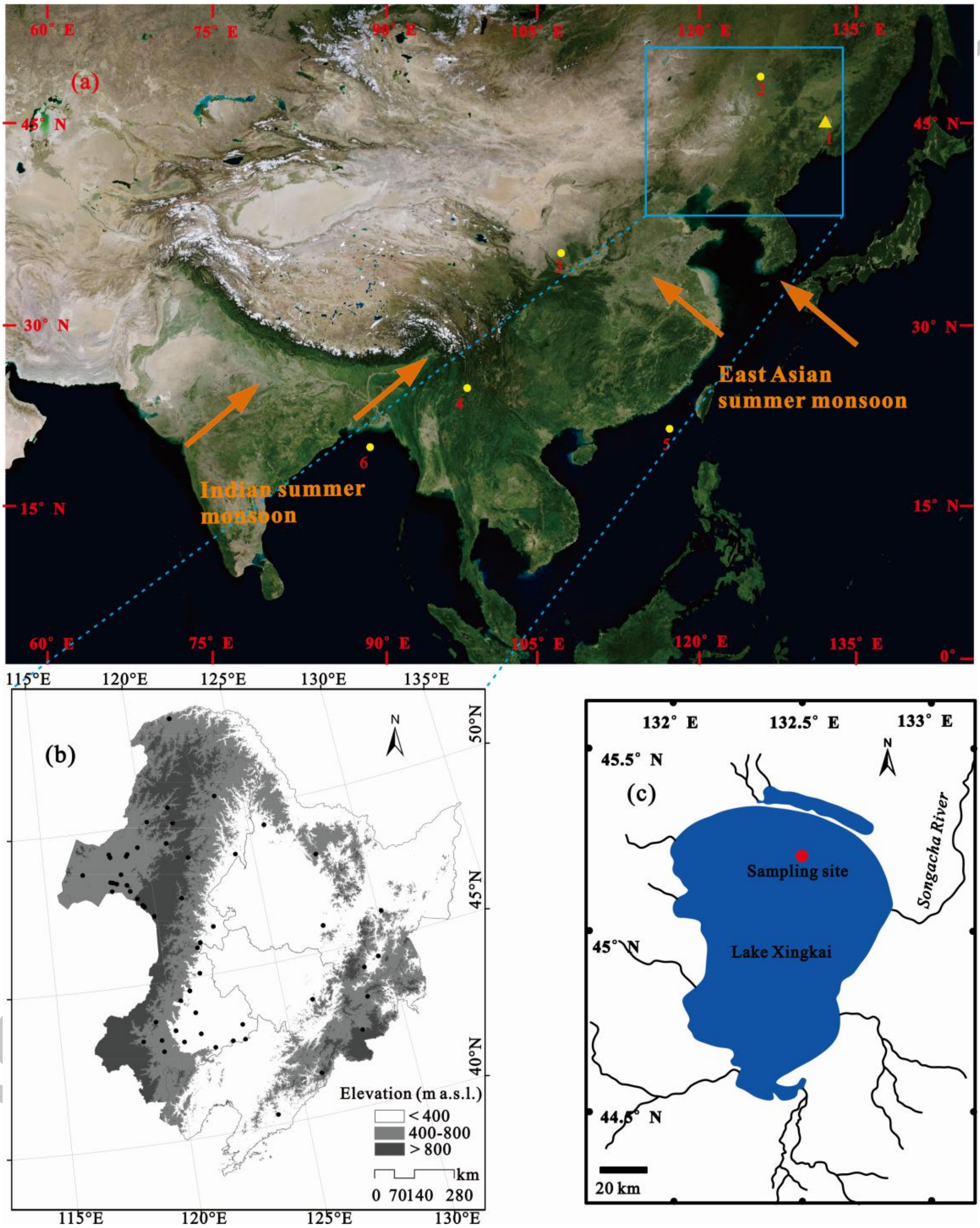

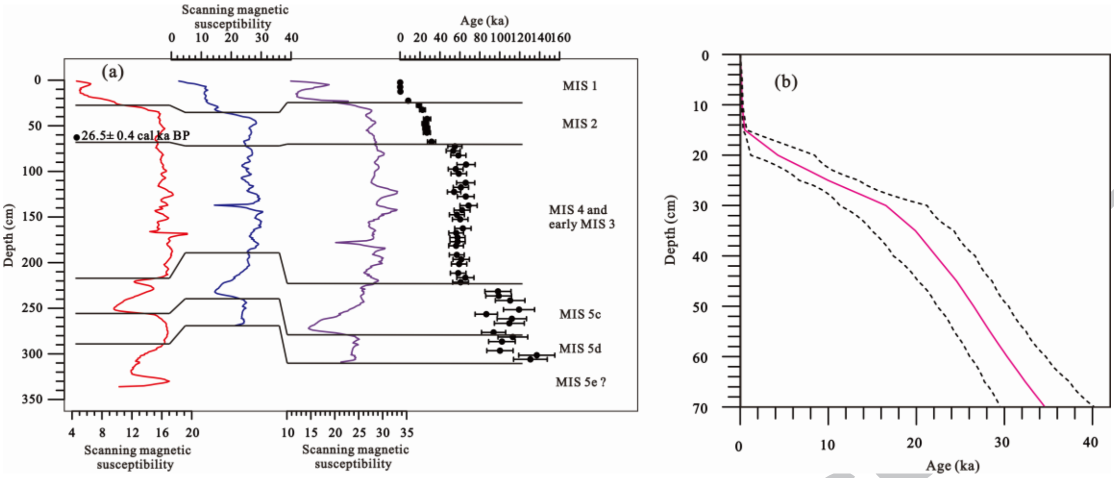
Scanning magnetic susceptibility
Age (ka)
(a)
Depth (cm)
26.5± 0.4 cal ka BP
MIS 1
MIS 2
MIS 4 and early MIS 3
MIS 5c
MIS 5d
MIS 5e ?
Scanning magnetic susceptibility
Scanning magnetic susceptibility
(b)
Depth (cm)
Age (ka)

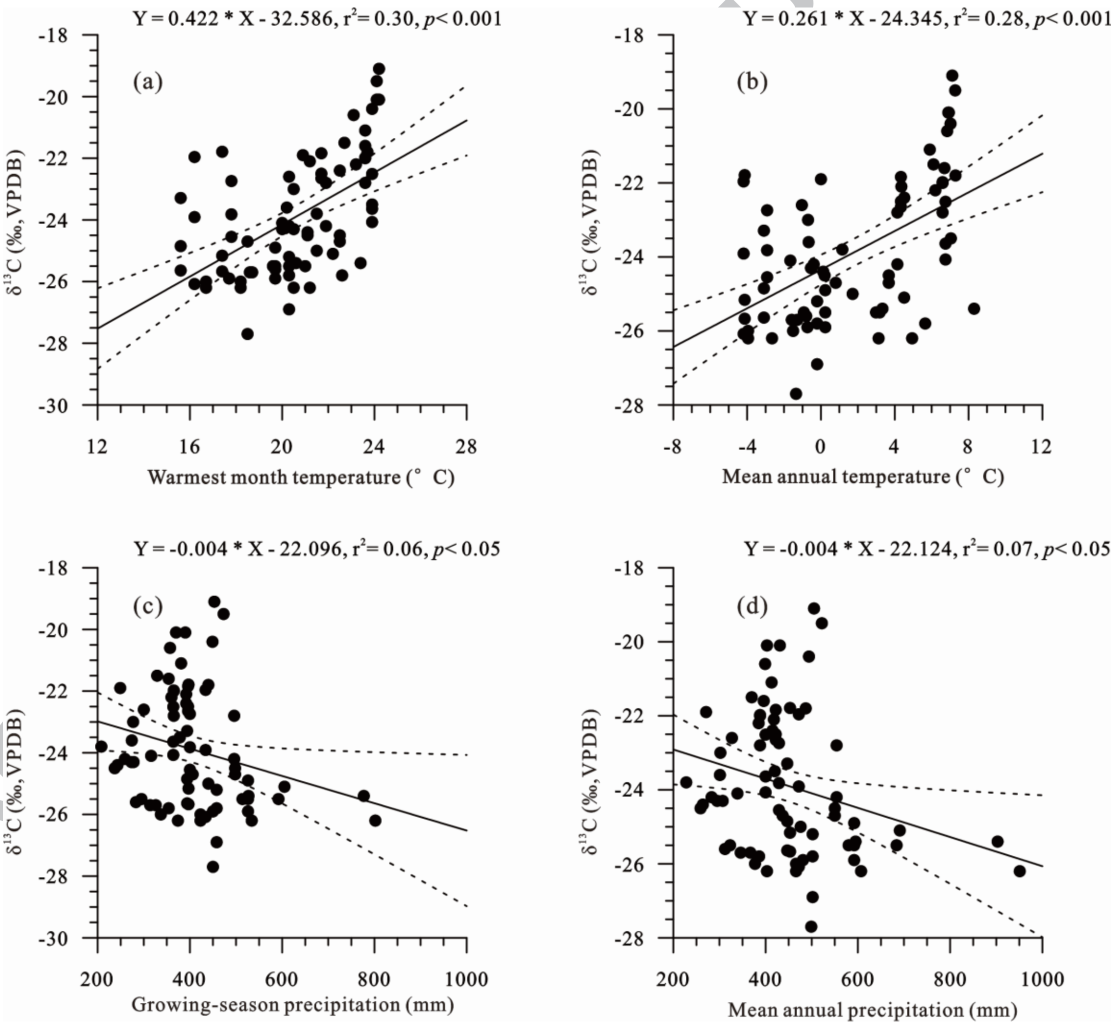
Y = 0.422 * X - 32.586, r² = 0.30, p < 0.001
(a)
δ13C (‰, VPDB)
Warmest month temperature (° C)
Y = 0.261 * X - 24.345, r² = 0.28, p < 0.001
(b)
δ13C (‰, VPDB)
Mean annual temperature (° C)
Y = -0.004 * X - 22.096, r² = 0.06, p < 0.05
(c)
δ13C (‰, VPDB)
Growing-season precipitation (mm)
Y = -0.004 * X - 22.124, r² = 0.07, p < 0.05
(d)
δ13C (‰, VPDB)
Mean annual precipitation (mm)

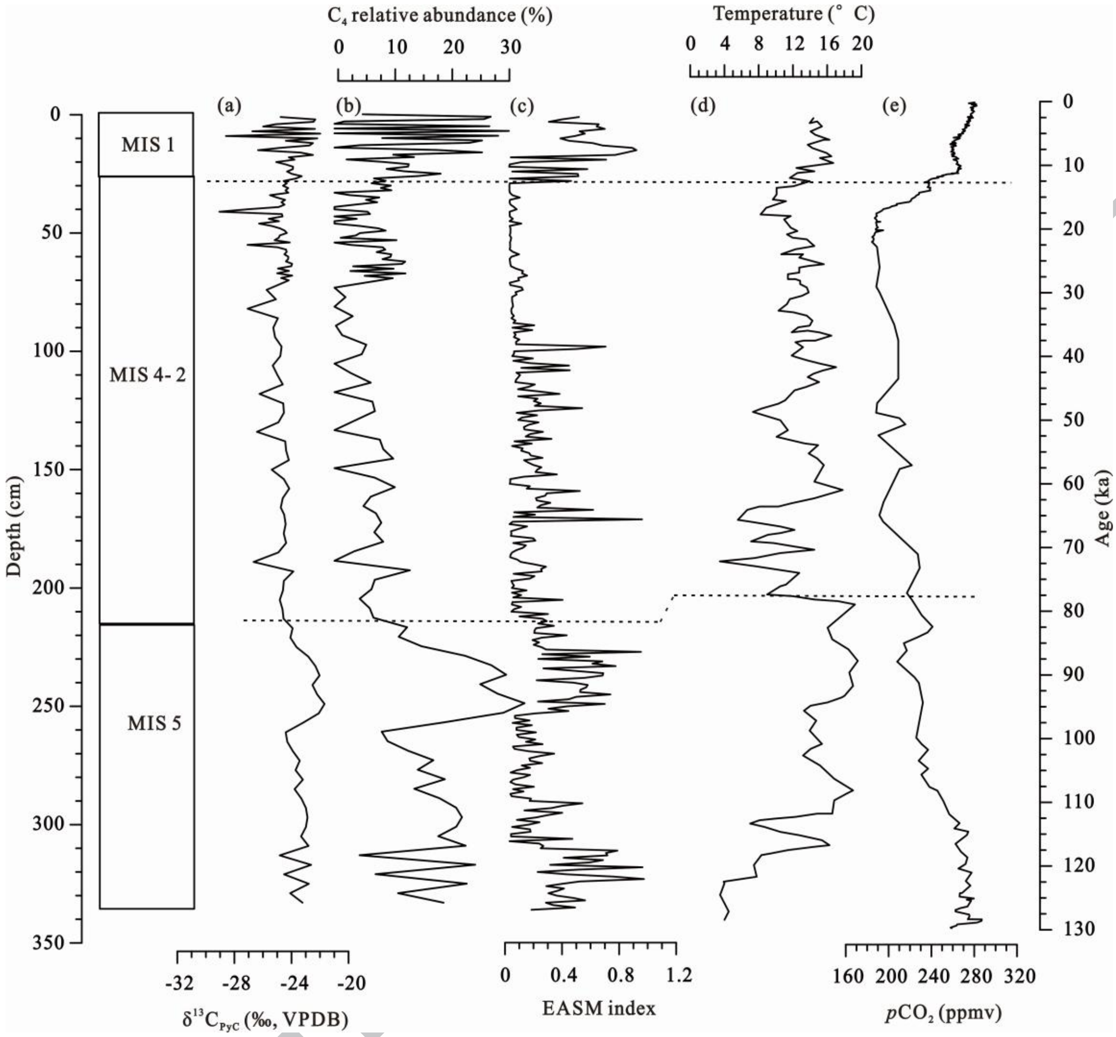
C4 relative abundance (%)
0 10 20 30
Temperature (° C)
0 4 8 12 16 20
(a)
(b)
(c)
(d)
(e)
MIS 1
MIS 4- 2
MIS 5
Depth (cm)
0
50
100
150
200
250
300
350
Age (ka)
0
10
20
30
40
50
60
70
80
90
100
110
120
130
-32 -28 -24 -20
δ13CPyC (‰, VPDB)
0 0.4 0.8 1.2
EASM index
160 200 240 280 320
pCO2 (ppmv)

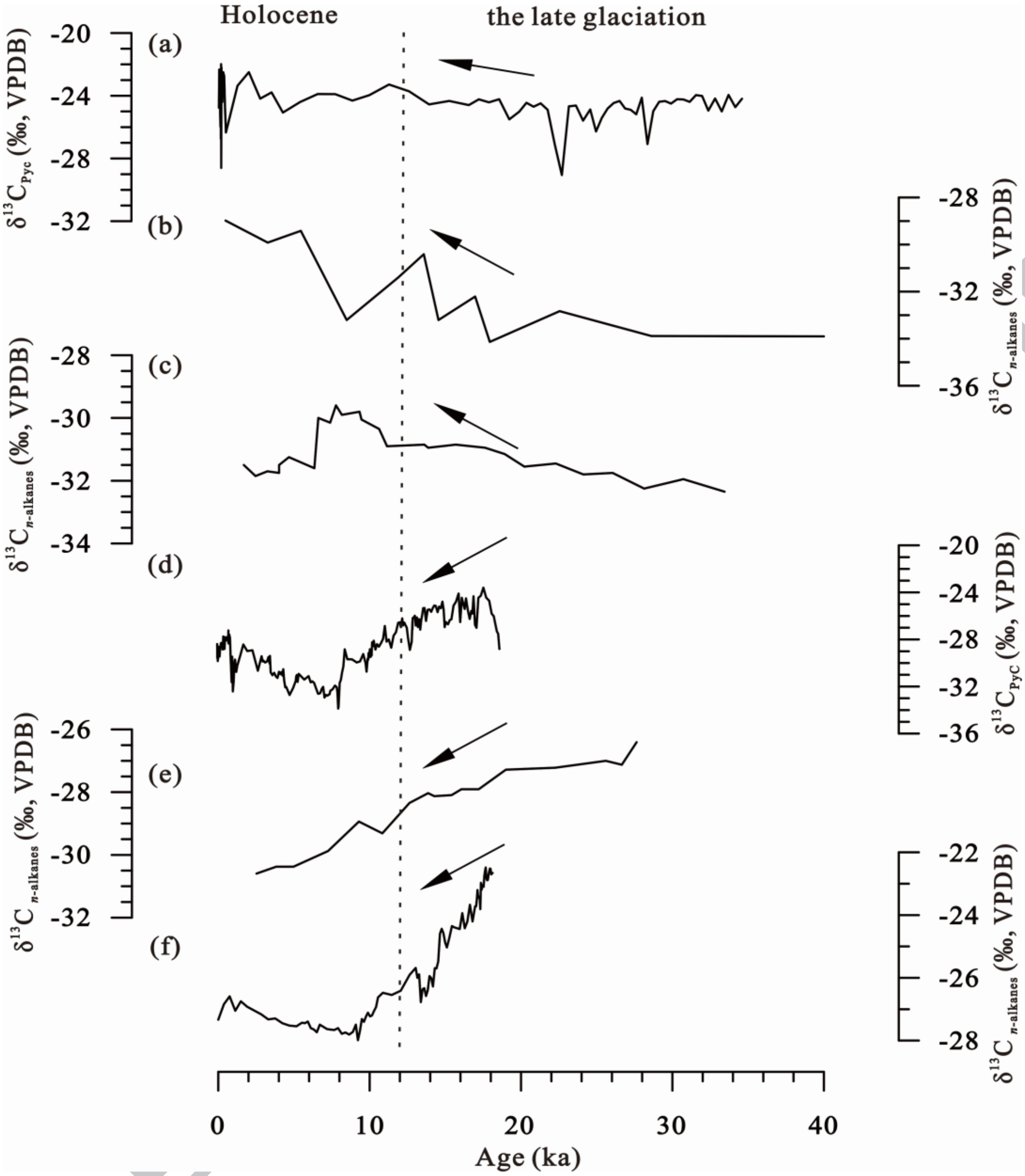

Holocene
the late glaciation
(a)
(b)
(c)
(d)
(e)
(f)
$\delta^{13}C_{Pyc}$ (‰, VPDB)
$\delta^{13}C_{n\text{-alkanes}}$ (‰, VPDB)
$\delta^{13}C_{PyC}$ (‰, VPDB)
Age (ka)

Highlights

- $\delta^{13}C$ of surface soil organic matter significantly influenced by temperature.
- $\delta^{13}C$ of pyrogenic carbon increased during the interglaciations in northeast China.
- Different climatic implication of $\delta^{13}C$ record between middle and low latitude.